Surface enhanced Raman scattering of p -aminothiophenol self-assembled monolayers in sandwich structure fabricated on glass

Yuling Wang, Hongjun Chen, Shaojun Dong, and Erkang Wang

Citation: The Journal of Chemical Physics **124**, 074709 (2006); doi: 10.1063/1.2172591

View online: http://dx.doi.org/10.1063/1.2172591

View Table of Contents: http://scitation.aip.org/content/aip/journal/jcp/124/7?ver=pdfcov

Published by the AIP Publishing

Surface enhanced Raman scattering of *p*-aminothiophenol self-assembled monolayers in sandwich structure fabricated on glass

Yuling Wang, Hongjun Chen, Shaojun Dong,[a),b)] and Erkang Wang[a),c)]
State Key Laboratory of Electroanalytical Chemistry, Changchun Institute of Applied Chemistry, Chinese Academy of Science, Changchun 130022, Jilin, People's Republic of China and Graduate School of the Chinese Academy of Sciences, Beijing 100039, People's Republic of China

(Received 12 August 2005; accepted 12 January 2006; published online 17 February 2006)

A sandwich structure consisting of Ag nanoparticles (NPs), *p*-aminothiophenol (*p*-ATP) self-assembled monolayers (SAMs), and Ag NPs was fabricated on glass and characterized by surface enhanced Raman scattering (SERS). The SERS spectrum of a *p*-ATP SAM in such sandwich structure shows that the electromagnetic enhancement is greater than that on Ag NPs assembled on glass. The obtained enhancement factors (EF) on solely one sandwich structure were as large as $6.0\pm0.62\times10^4$ and $1.2\pm0.62\times10^7$ for the $7a$ and $3b(b_2)$ vibration modes, respectively. The large enhancement effect of *p*-ATP SAMs is likely a result of plasmon coupling between the two layers of Ag NP (localized surface plasmon) resonance, creating a large localized electromagnetic field at their interface, where *p*-ATP resides. Moreover, the fact that large EF values ($\sim1.9\pm0.7\times10^4$ and $9.4\pm0.7\times10^6$ for the $7a$- and b_2-type vibration modes, respectively) were also obtained on a single sandwich structure of Au NPs/*p*-ATP SAMs/Ag NPs in the visible demonstrates that the electromagnetic coupling does not exist only between Ag NPs but also between Au and Ag NPs. The lower EF values on Au-to-Ag NPs compared to those on Ag-to-Ag NPs demonstrate that the Au-to-Ag coupling must be less effective than the Ag-to-Ag coupling for the induction of SERS in the visible. © *2006 American Institute of Physics*. [DOI: 10.1063/1.2172591]

INTRODUCTION

Since the first discovery of surface enhanced Raman scattering (SERS) of pyridine on the electrochemically roughened Ag electrode by Fleischmann *et al.* in 1974,[1] SERS has attracted substantial interest because of its potential applications in trace analysis,[2–5] nanoscience,[6–10] and biological science.[11–14] Currently, there are two separated mechanisms to describe the overall SERS effect: electromagnetic effect (EM) and chemical effect (CM). EM is regarded as a long-range effect, in which the localized electromagnetic field plays the most roles in SERS,[15–18] while CM is the interaction of the adsorbate adsorbed on the metal surface with the metal, such as the charge transfer of the adsorbate with the metal.[19–21]

Since the first introduction of the roughened Ag electrode as a SERS active substrate, much attention has turned to the metallic colloid system because of their strong light scatterings and tunable optical properties.[22,23] Early in 1995, Freeman *et al.* have assembled metal nanoparticles (NPs) such as Au and Ag on silane-modified glass to exploit the novel properties of nanosized particles and to obtain a stable and reproducible substrate for SERS.[24] And in 1997, Nie and Emery reported single molecule detection (SMD) by SERS on single aggregated Ag NPs.[25] The SERS enhancement factors can reach as large as 10^{14}. Such large enhancement factors may be derived from the electromagnetic field in which probe molecules reside in the junction of the two aggregated Ag NPs according to Michaels *et al.*[26] All these reports enhance the interest of the metallic colloid system in SERS applications. Compared with the bulk metal, nanosized metal particles have special physical, optical, and chemical properties. As reported, as the surface plasmons are localized in a confined volume, such as in nanosized metal particles, the localized electromagnetic field can be remarkably amplified.[27–29] Under resonance conditions, Raman scattering can be enhanced by the localized surface plasmon (LSP) resonance.[30,31] Zheng *et al.* have successfully applied this property of the nanosized silver particles and fabricated assemblies of nanosized Ag particles, *p*-aminothiophenol (*p*-ATP), and the smooth macroscopic Ag substrate to study the SERS spectra of *p*-ATP in such structure.[32] The proposed enhancement of the spectrum of *p*-ATP in the assemblies was ascribed to the electromagnetic coupling between the Ag NPs and the smooth macroscopic Ag surface, the so-called LSP-surface plasmon polariton (SPP) coupling. Recently, Orendorff *et al.* fabricated a sandwich architecture of a smooth macroscopic Au substrate, 4-mercaptobenzoic acid Self-assembled monolayers (SAMs), and Au NPs with various shapes.[33] Large enhancement factors (10^7–10^9) were obtained on the SERS spectra of 4-mercaptobenzoic acid (4-MBA) SAMs and were considered to be derived mainly from the electromagnetic coupling of LSP-SPP between the nanosized Au particles and the smooth Au substrate. On the other hand, Kim and co-workers have systematically reported that a SERS spectrum could be obtained for *p*-ATP

[a)]Authors to whom correspondence should be addressed. Fax: +86-431-5689711.
[b)]Electronic mail: dongsj@ciac.jl.cn
[c)]Electronic mail: ekwang@ciac.jl.cn

adsorbed onto macroscopically smooth Au and Cu surfaces by assembling nanosized Ag and Au particles thereon. The enhancement of the SERS spectra of *p*-ATP was ascribed to an EM coupling between the Ag or Au NPs and the surface of the Au or Cu substrate, most probably due to the interactions of LSP-SPP.[34,35] Keating *et al.* have studied the SERS spectra of cytochrom *c* in metal/cytochrom *c*/metal sandwich in solution and proposed that the heightened electromagnetic fields appeared between the metal NPs.[36]

However, little attention has been paid to the interaction of two layers of nanosized metallic particles on a solid substrate where coupling molecule SAMs reside. The sandwich structure on the solid substrate may have better stability and reproducibility than that in solution because of the controllable assembly process. In this paper, such sandwich structure consisting of Ag NPs, *p*-ATP SAMs, and Ag NPs was fabricated on glass and characterized by SERS. *p*-ATP was chosen as the coupling molecule owing to its bifunctional properties. The electromagnetic coupling between the two layers of Ag NPs is considered to be responsible for the enhancement of the spectrum of *p*-ATP SAMs in such sandwich structure. Ideally, each coupling molecule may reside in the junction of two layers of Ag NPs fabricated on glass. Such structure is estimated to produce large enhancement factors according to Michaels *et al.*[26] The obtained enhancement factor (EF) values on each one of the Ag-to-Ag NP sandwich structure were as large as $6.0\pm0.62\times10^4$ and $1.2\pm0.62\times10^7$ for 7*a* and b_2-type vibration modes based on the theoretical calculation. Such electromagnetic coupling was assumed to exist not only between the Ag-to-Ag NPs but also between the Au-to-Ag NPs. Here, the SERS spectrum of *p*-ATP in Au NPs/*p*-ATP SAMs/Ag NPs was also reported to elucidate the electromagnetic coupling effect between two layers of metal NPs. Large EF values were also obtained on this sandwich structure on glass in the visible. It is well known that Au has lower EF values in the visible[37] and many attempts to obtain composite particles by depositing Ag on preformed Au particles have been extensively carried out.[38,39] So we hope our report could have some contributions to the research of the SERS enhancement mechanism on the Au surface.

EXPERIMENT

Chemicals

3-mercaptopropyltrimethoxysilane (3-MPTMS) and *p*-ATP from Aldrich Chemical Co. were used without further purification. The other chemicals were all of regent grade. An aqueous solution was prepared using distilled de-ionized water.

Preparation of colloidal Ag NPs and Au NPs

Ag sols were prepared by aqueous reduction of $AgNO_3$ with trisodium citrate following the method of Lee and Meisel.[40] Briefly, silver nitrate (18 mg) was suspended in 100 mL of de-ionized water at 45 °C and rapidly heated to boiling point before a 1% solution of trisodium citrate (2 mL) was added under vigorous stirring. The solution was held at boiling point for 90 min until continuous stirring upon cooling. The volume was made up to 100 mL with de-ionized water. Au NPs with sizes comparable to those of Ag NPs were prepared by aqueous reduction of $HAuCl_4$ with trisodium citrate according to Frens's method.[41] That 50 mL of 0.01% $HAuCl_4$ solution was heated to boiling point, and 0.3 mL of 1% trisodium citrate was added. The solution was kept boiling for 5 min. The field emission scanning electron microscopy (FE-SEM) showed that the average diameter was ~70 nm for both NPs.

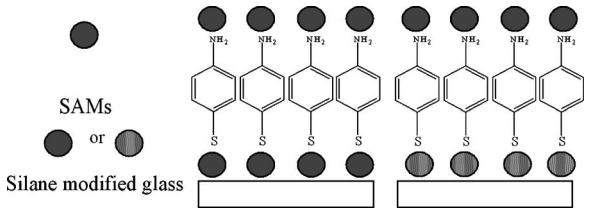

FIG. 1. Scheme of Ag NPs/*p*-ATP SAMs/Ag NPs and Au NPs/*p*-ATP SAMs/Ag NPs sandwich structures fabricated on silane modified glass for SERS of *p*-ATP (● and ● represent Ag and Au NPs, respectively).

Methods of fabricating sandwich structures on silane modified glass

Ag or Au NPs were modified on glass in the following procedure: First, a glass slice was cleaned in a heated piranha solution (75% H_2SO_4/25% H_2O_2) for 30 min and then sonicated in water and ethanol for 20 min, respectively. Second, the clean glass slice was immersed in 2% 3-MPTMS ethanol for 6 h to make the glass silane modified. And third, the modified glass was immersed in Ag sols and Au sols for 6 h, respectively, resulting in the Ag and Au NPs attached to the silane modified glass, finally forming a layer of metal NPs on the silane modified glass.

Sandwich structures were fabricated, as indicated in Fig. 1. The glass modified by a layer of Ag NPs was immersed in $10^{-4}M$ *p*-ATP ethanol solutions for 6 h to form *p*-ATP SAMs, and then the surface was thoroughly washed with ethanol and water and immersed in Ag sols overnight. Then the sandwich structure consisting of Ag NPs, *p*-ATP SAMs, and Ag NPs was formed. The sandwich structure of Au NPs/*p*-ATP/Ag NPs can be obtained in the same way.

Instruments

The conductive indium tin oxide (ITO) films with attached Ag and Au NPs were imaged by an XL30 ESEM FEG field emission scanning electron microscopy (FEI Company). The graphs of sandwich structures of Ag NPs/*p*-ATP/Ag NPs and Au NPs/*p*-ATP/Ag NPs were also obtained by FE-SEM.

SERS spectra were recorded with a Renishaw 2000 equipped by an Ar^+ ion laser giving the excitation line of 514.5 nm and an air cooling charge coupled device (CCD) as the detector (Renishaw Co., UK). The Raman band of a silicon wafer at 520 cm^{-1} was used to calibrate the spectrometer.

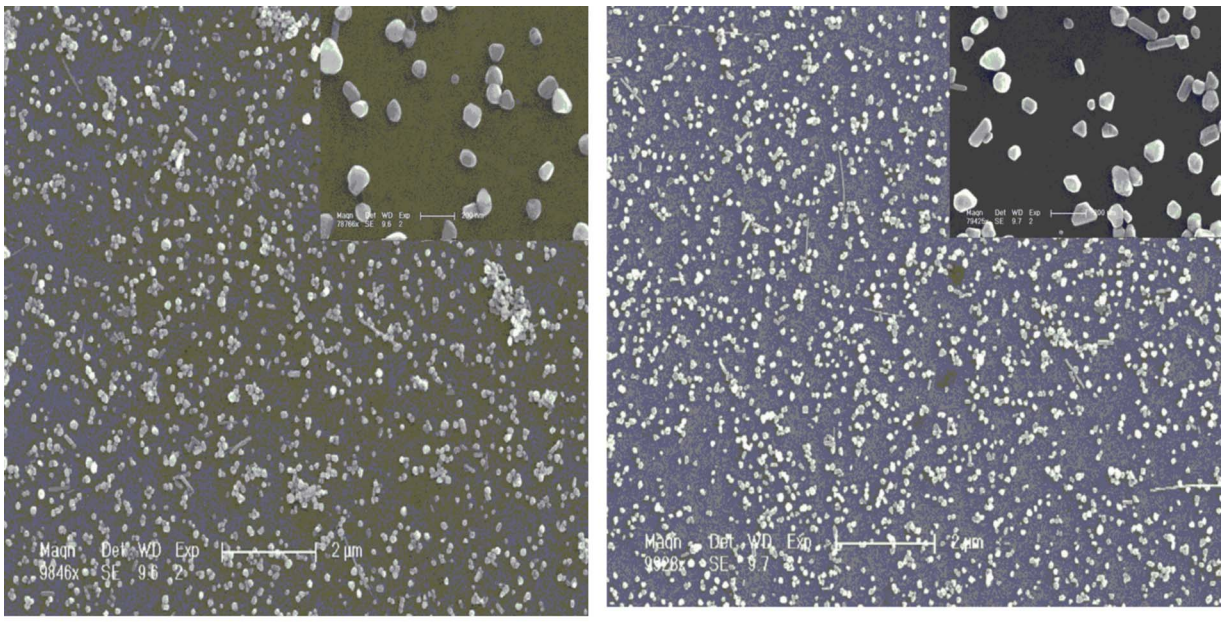

FIG. 2. FE-SEM images of Ag NPs assembled on glass (a) and in the Ag NPs/*p*-ATP SAMs/Ag NPs sandwich structure (b). Inset shows the high magnification of the SEM images.

RESULTS AND DISCUSSIONS

p-ATP was chosen as the coupling molecule because *p*-ATP is a bifunctional molecule whose -SH group is easily cleavaged to form a metal–S bond when adsorbed on a metal surface, and the protonated amino group can adsorb on the metal surface through the electrostatic force between the protonated amino group and the negative charged metal NPs.

Figure 2 gives the morphology of Ag NPs assembled on the silane modified glass and Ag NPs/*p*-ATP SAMs/Ag NPs on ITO by FE-SEM. Obviously, Ag NPs assembled on the silane modified ITO are distributed fairly uniformly on the surface. Although a few aggregates and some Ag nanorods can be observed (occupying ~5% of the total), most of the particles exist separately. The high magnification of FE-SEM is also shown in the inset of Fig. 2, which more clearly indicates the uniform distribution of Ag NPs. The obtained surface coverage of Ag NPs on glass was 19 particles/μm^2. (The high magnification of FE-SEM images is selected randomly and can represent the whole distribution of the NPs). The surface coverage of Ag NPs on ITO increased to 29 particles/μm^2 when the second layer of Ag NPs attached through electrostatic force between *p*-ATP and Ag NPs, as shown in Fig. 2(b), demonstrating that the sandwich structure of Ag NPs/*p*-ATP/Ag NPs was fabricated successfully. To evaluate more quantitatively the effectiveness of the second layer of Ag NPs for the induction of SERS by metal NPs-to-NPs, the number of Ag NPs that are formed in sandwich structures has been determined via the surface coverage, which was estimated to be 10 particles/μm^2. Considering the electrostatic repulsion of the colloid particles encapsulated by negatively charged citrate ions, Ag NPs should not cover fully the *p*-ATP on the first layer of Ag NPs and the maximum surface coverage attainable is ~50%, indicating that the interaction between Ag NPs in the second layer is not as strong as that between Ag NPs on glass in the first layer and that the influence to the SERS signal can be neglected. Therefore, the amount of *p*-ATP molecules which are situated in the two Ag NPs as well as the amount of *p*-ATP on only one Ag nanoparticle can be determined. According to the report by Kim and Yoon[34] and Kim and Lee[35] each *p*-ATP molecule occupies an area of ~0.2 nm^2. The amounts of *p*-ATP molecules that are actually sandwiched in the two Ag NPs and bound to only one Ag particle are 1.92×10^5 molecules/μm^2 and 1.78×10^5 molecules/μm^2, respectively. It is noteworthy that Ag NPs can be adsorbed on the mercaptosilane molecules even during the formation of the second layer of Ag NPs on *p*-ATP SAMs. However, because it is difficult to discern from the first layer of Ag NPs, the influence of these particles to the SERS signal can be neglected. In fact, the number of the sandwich structure will be lower than 10, which will result in relatively lower calculated EF values on sandwich structures.

Figure 3 shows the Raman spectrum of solid *p*-ATP and the SERS spectra of *p*-ATP SAMs on Ag NPs assembled on glass and in the Ag NPs/*p*-ATP SAMs/Ag NPs sandwich structure. The normal Raman spectrum of solid *p*-ATP is similar to that obtained on the literature.[42,43] In Fig. 3(c) there is a strong band that appeared at 238 cm^{-1}. On the basis of the fact that this band is enhanced upon the second layer of Ag NPs attached on *p*-ATP SAM, it may be reasonable to assign this band to the Ag–S stretching vibration. A similar band was also observed in the SERS spectrum of 6-mercaptopurine[44] and thiophenol[45] on the Ag surface. Considering the fact that there were no observed Raman peaks of MPTMS molecules when the first layers of Ag NPs assembled on the silane modified glass and no Raman peaks of MPTMS were observed on Au electrode/MPTMS/Ag NPs

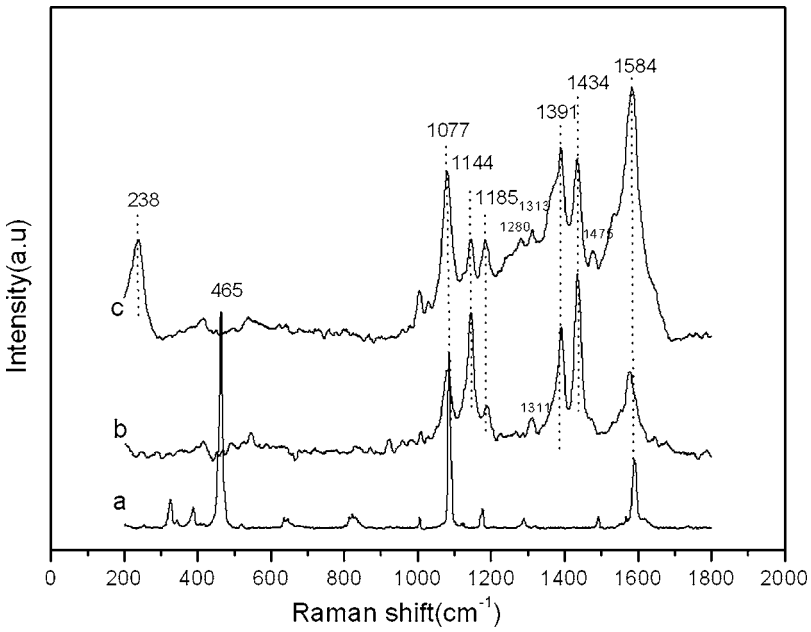

FIG. 3. Raman spectrum of solid *p*-ATP (a), SERS spectra of *p*-ATP on the Ag NP modified glass (b) and in the Ag NPs/*p*-ATP SAMs/Ag NPs sandwich structure (c).

in our previous study,[46] the sulfur atom should belong to *p*-ATP rather than to silane molecules. In Fig. 3(b), the vibration of the Ag–S bond is very weak, which proves that *p*-ATP adsorbs on the first layer of the surface of Ag NPs through the Ag–S bond.[47] A big change in the relative intensity of the vibration bands was also observed between Figs. 3(b) and 3(c). In Fig. 3(b), the SERS spectrum of *p*-ATP on the Ag NP modified glass is similar to that on the Ag surface reported,[32,42] in which the intensities of four b_2 modes at 1580, 1436, 1390, and 1144 cm^{-1} and of one a_1 mode at 1080 cm^{-1} increase compared with the Raman spectrum of solid *p*-ATP, as shown in Fig. 3(a). The corresponding intensity of the b_2 mode increases, which is associated with the charge transfer of the metal to the adsorbed molecules. As reported, the obvious enhancement of b_2 modes in the visible was interpreted in terms of a metal-to-molecule charge transfer (CT) theory,[32,42] while EM cannot be neglected because the a_1 mode (1080 cm^{-1}) was also enhanced. The electromagnetic effect may be derived from the localized surface plasmon resonance of the Ag NPs assembled on glass. In Fig. 3(c) the electromagnetic field around the Ag NPs is changed when the second layer of Ag NPs attached on the *p*-ATP SAMs because of the electromagnetic coupling between the two layers of Ag NPs. This kind of electromagnetic coupling can be proven by the great enhancement of $7a_1$ at 1077 cm^{-1}, whose relative intensity increases more than that of b_2 modes compared with Fig. 3(b). In Fig. 3(b), the intensity ratio of I_{1080}/I_{1434} is 0.375, while in Fig. 3(c) the ratio is improved to 1.625. Cao *et al.*[18] and Wang *et al.*[48] have reported that the enhancement of the a_1 only comes from the electromagnetic effect: its intensity was independent of the applied electrochemical potential. Osawa *et al.* have also investigated the vibration of a_1 and b_2 with the applied potentials and found that the bands assigned to b_2 species greatly decreased in intensity and disappeared completely around −0.4 V vs SCE, while the $\nu_7(a_1)$ at 1077 cm^{-1} is almost insensitive to the potential change.[42] It also illustrated that the $\nu_7(a_1)$ is derived solely from the electromagnetic effect though it is difficult to figure out EM from CT effect. Therefore, the marked improvement of the relative intensity of $\nu_{CS}(7a_1)$ may prove the strong electromagnetic coupling between the two layers of Ag NPs. This enhancement also illustrates that the orientation of *p*-ATP adsorbed on the first layer of Ag NPs is vertical on the Ag surface.[43] Oteral and co-workers have proposed that different relative intensities in the SERS spectra of aromatic molecules such as pyrazine on Ag, Au, Cu, and Ni depended on the nature of the metal.[49–51] Cao *et al.* have also investigated the SERS of *p*-ATP on the Au(core)/Cu(shell) surface and proposed the difference in the relative intensity of the SERS spectra of *p*-ATP on the Au surface and Au(core)/Cu(shell) can be ascribed to the chemical effect.[18] But in our system, the substrate is the same metal of Ag, and then the nature of the metal cannot influence the chemical effect of the SERS spectra of *p*-ATP. Therefore, the difference in relative intensity should be ascribed to the electromagnetic coupling effect, which is derived from the two layers of the surface Ag NPs on the silane modified glass. The appearance of the Ag–S vibration proves that the second layer of Ag NPs increases the electromagnetic field of the first layer of Ag NP's surrounding and makes the electromagnetic enhancement of the Ag NPs to *p*-ATP increase greatly, as indicated in Fig. 3(c). As reported, this structure is more approachable than the theoretical model that an analyte molecule positioned between two noble metal NPs can be enhanced greatly.[52] So one of the most interesting possibilities about the method of fabricating sandwich structures on glass is to achieve a kind of electromagnetic coupling effect between the two layers of metal NPs through controlling the assembly process, and this effect is known to give a dominant contribution to the SERS efficiency.[49] Therefore, large EF values are estimated to exist in such sandwich structure. It is notable that the spectra features in our system are much different from those obtained by Zheng *et al.*, which are obtained at 1064 nm excitation.[32] If the influence of the excitation line is neglected, the differ-

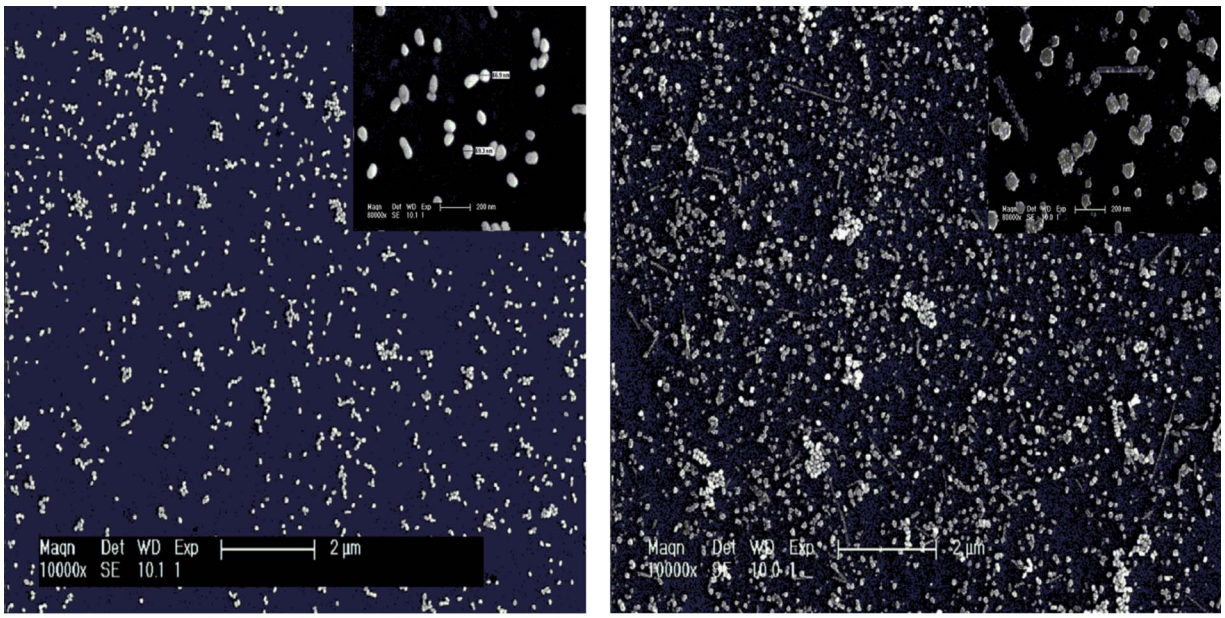

FIG. 4. FE-SEM images of Au NPs assembled on glass (a) and in the Au NPs/*p*-ATP SAMs/Ag NPs sandwich structure (b).

ence may be derived from the substrate of the smooth macro Ag surface and nanosized Ag surface. We assume that there are differences between the LSP-SPP coupling and the interaction of the LSP coupling.

To inquire the enhancement effect of *p*-ATP on these structures quantitatively, the EF values of *p*-ATP in the sandwich structure were calculated according to the references.[33,37,53–56] The EF was defined as

$$\mathrm{EF} = \frac{I_{\mathrm{SERS}}/N_{\mathrm{ads}}}{I_{\mathrm{bulk}}/N_{\mathrm{bulk}}},$$

where I_{SERS} stands for the intensity of a vibrational mode in the SERS spectrum of *p*-ATP and I_{bulk} for the intensity of the same vibrational mode in the Raman spectrum from the solution phase or solid sample. Both of these intensities can be directly obtained from the experiment. To more objectively evaluate the EF, the EF values for the $7a$- and b_2-type modes are determined on the Ag NPs and sandwich structure of Ag-to-Ag NPs. For all the spectra, the intensity of the $\nu_{7a}(a_1)$ at $\sim$1080 cm^{-1} and that of the $3b(b_2)$ at $\sim$1390 cm^{-1} were used to calculate the EF values. All spectra were normalized for acquisition time and laser power. N_{ads} is the number of surface adsorbed *p*-ATP molecules within the laser spot. This value can be obtained according to the method proposed by Orendorff *et al.*,[33] which is

$$N_{\mathrm{ads}} = N_d A_{\mathrm{laser}} A_N/\sigma,$$

where N_d is the number density of the NPs, A_{laser} is the area of the focal spot of the laser, A_N is the NP's footprint area, and σ is the surface area occupied by an adsorbed *p*-ATP molecule. N_d and A_N can be obtained from the SEM images in Fig. 2(a), and A_{laser} can be obtained from the diameter of the laser spot ($\sim$1 μm). According to the report by Kim and Yoon[34] and Kim and Lee[35] each *p*-ATP molecule occupies $\sim$0.20 nm^2 on full coverage of Au, indicating that σ can be adopted as $\sim$0.20 nm^2/molecule. Then the total number of surface adsorbed molecules (N_{ads}) on Ag NPs assembled on the silane modified glass within the illuminated laser spot can be obtained at 2.9×10^5. N_{bulk} is the molecule number of the solid *p*-ATP in the laser illumination volume. In our experiment, the laser spot of 1 μm in diameter and the penetration depth ($\sim$16.5 μm) of the focused laser beam are used. Taking the density of the solid *p*-ATP (1.18 $\mathrm{g/cm}^3$) into account,[57] N_{bulk} was calculated to be about 7.3×10^{10} within the illuminated laser light. Considering the fact that the intensity ratios of the ring $7a$ bands at $\sim$1080 cm^{-1} and b_2-type vibration mode at $\sim$1390 cm^{-1} in Figs. 3(a) and 3(b) were measured to be 0.49 and 122.7, respectively, normalized with respect to the absolute intensity of a silicon wafer, EF values on Ag NPs on glass can be obtained at $1.2\pm0.62\times10^5$ and $3.1\pm0.62\times10^7$ for $7a$- and b_2-type vibration modes, respectively. (It is noticeable that the calculated error is ascribed to the Nd and the area of the NPs because they are approximately calculated according to the SEM images). Recalling the fact that the number of the Ag NPs illuminated by laser light was 15 particles, the EF values derived solely from a single Ag NP are then obtained at $8.4\pm0.62\times10^3$ and $2.1\pm0.62\times10^6$ for ring $7a$- and b_2-type vibration modes, respectively. According to the SEM images, the amount of *p*-ATP molecules that are actually sandwiched can be achieved at 1.92×10^5 molecules/$\mu\mathrm{m}^2$ when the second layer of Ag NPs is attached. If the contribution of the other nine single Ag NPs on the second layer is considered, the total EF values of about $2.6\pm0.62\times10^5$ will be obtained. Recalling the fact that the EF values on a single Ag NP are $8.4\pm0.62\times10^3$, then the EF values on each one of the sandwich structures will be achieved at $3.0\pm0.62\times10^4$, which are two to three times greater than those obtained on Ag NPs on glass. However, assuming that the SERS signal is derived solely from the sandwich structures, the EF values on the

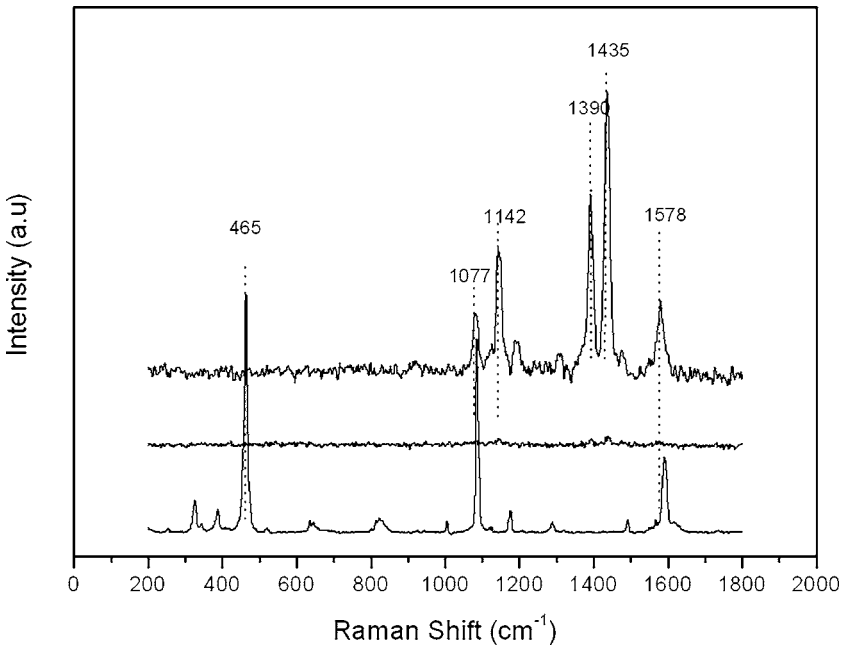

FIG. 5. Raman spectrum of the solid *p*-ATP (a), SERS spectra of *p*-ATP on the Au NP modified glass (b) and in NPs/*p*-ATP SAMs/Ag NPs sandwich structure (c).

sandwich structures will be as large as $4.6\pm0.62\times10^5$ and $9.0\pm0.62\times10^7$ for the $7a$- and b_2-type vibration modes, respectively. Considering the fact that the number of sandwich structures illuminated by laser light was 7.85 particles, the EF values derived solely from one sandwich structure are then to be $6.0\pm0.62\times10^4$ and $1.2\pm0.62\times10^7$ for ring $7a$- and b_2-type vibration modes, respectively, which are seven to eight times greater than those obtained on a single Ag NP on glass. In fact, the EF values on the sandwich structure will be far greater than the obtained values because some Ag NPs may be anchored to the mercaptosilane molecules even during the formation of the second layer of Ag NPs on *p*-ATP SAMs, which have less contribution to the SERS signal of *p*-ATP in the sandwich structure. Although the EF values are not excessively large, it clearly suggests that the sandwich structure can provide a hot spot for the induction of the SERS of *p*-ATP via the electromagnetic coupling between two layers of Ag NPs. It is noteworthy that the EF values for the b_2-type mode are ~100 higher than those for the $7a$ mode, which may be attributed to the chemical effect because of the formation of the strong Ag–S bond. If the EF values of *p*-ATP on Ag NPs assembled on glass is attributed mainly to the localized surface plasmon resonance of the Ag NPs, the larger EF values of *p*-ATP SAMs in the sandwich structure were attributed mainly to the electromagnetic coupling between the two layers of Ag NPs localized in the two ends of *p*-ATP SAMs.

Another piece of direct evidence comes from another SERS measurement of *p*-ATP SAMs, corresponding to the coupling layer between Ag and Au NPs. The electromagnetic coupling is assumed to exist between the Au and Ag NPs. FE-SEM images of Au NPs with similar sizes of Ag and Au NPs/*p*-ATP SAMS/Ag NPs were obtained, as indicated in Fig. 4. Obviously, Au NPs assembled on the silane modified ITO distribute fairly uniformly on the surface. Most of the particles exist separately and a few aggregates can be ob-

TABLE I. Assignments and wave number positions (cm^{-1}) for the Raman and SERS spectra of *p*-aminothiophenol.

Solid *p*-ATP	*p*-ATP/Ag	Ag/*p*-ATP/Ag	Ag/*p*-ATP/Au	Assignments[a]
1591 (*s*)				νCC, $8a(a_1)$
	1580 (*m*)[b]	1584 (*s*)	1578 (*m*)	νCC, $8b(b_2)$
1493 (*w*)	1470 (vw)	1479 (*w*)	1475 (*w*)	
1425 (vw)	1436 (*s*)	1434 (*m*)	1435 (*s*)	$\nu_{CC}+\delta_{CH}$, $19b(b_2)$
1369 (vw)	1390 (*m*)	1391 (*m*)	1390 (*m*)	$\delta_{CH}+\nu_{CC}$, $3b(b_2)$
	1311 (*w*)	1313 (*w*)	1310 (*w*)	$\nu_{CC}+\delta_{CH}$, $14b(b_2)$
1288 (*w*)	1280 (*w*)	1280 (*w*)		ν_{CH}, $7a(a_1)$
1179 (*m*)	1188 (*w*)	1185 (*m*)	1192 (*w*)	δ_{CH}, $9a(a_1)$
1126 (*w*)	1144 (*s*)	1144 (*m*)	1142 (*s*)	δ_{CH}, $9b(b_2)$
1084 (vs)	1080 (*m*)	1077 (*s*)	1077 (*m*)	ν_{CS}, $7a(a_1)$
465 (vs)				γ_{CCC}, $7a(a_1)$
		238 (*s*)		ν_{Ag-S}

[a]Assignments for the SERS spectra of *p*-ATP from Refs. 32, 41, and 43.
[b]Relative intensities (*s*, strong; *m*, middle; *w*, weak; vw, very weak; and vs, very strong).

served. According to the high magnification of the FE-SEM, as shown in the inset of Fig. 4, the surface coverage of Au NPs is approximately 20 particles/μm^2, which is similar to that of Ag NPs. The increase of the surface coverage of metal NPs to 32 particles/μm^2, as shown in Fig. 4(b), demonstrates that the sandwich structure of Au NPs/*p*-ATP/Ag NPs was fabricated successfully. It is well known that Au surface shows lower EF values in the visible.[37] Therefore, there is a weak Raman signal of *p*-ATP on Au NPs detected in the visible, as shown in Fig. 5(b). But when a layer of Ag NPs was immobilized on it, the SERS spectrum of *p*-ATP is evident, as indicated in Fig. 5(c). With a similar calculation, EF values on a single sandwich structure of Au-to-Ag NPs can be achieved at $1.9\pm0.7\times10^4$ and $9.4\pm0.7\times10^6$ for $7a$ and $3b(b_2)$ vibration modes, respectively. Large EF values are assumed to be derived from the strong electromagnetic coupling between Au and Ag NPs, which also suggests that the sandwich structure can provide a hot spot for the induction of SERS via the electromagnetic coupling. Meanwhile, the obtained EF values are compared with those obtained on Ag NPs assembled on the silane modified glass. Assuming that the interactions between the Ag NPs in the second layer are very strong, then the obtained EF values should be the same as those obtained on Ag NPs on glass or lower than those obtained on them because the maximum surface coverage of the second layer (12 particles/μm^2) is lower than that of the first layer of Ag NPs on glass (19 particles/μm^2). However, the obtained EF values on the sandwich structure of Au-to-Ag are two to three times higher than those obtained on Ag NPs on glass, indicating that the interactions between the Ag NPs in the second layer would be very weak and can be ignored. Herein, the large EF values on the sandwich structure of Au-to-Ag NPs would be mainly ascribed to the strong electromagnetic coupling between Ag and Au NPs. It has to be mentioned that EF values on the sandwich structure of Au-to-Ag NPs are lower than those obtained on the sandwich structure of Ag-to-Ag NPs, which demonstrates that the Au-to-Ag coupling should be less effective than the Ag-to-Ag coupling for the induction of SERS, corresponding to the results reported by Kim and Yoon.[34] On the other hand, the SERS spectra features of *p*-ATP in the Au NPs/*p*-ATP/Ag NPs sandwich structure are similar with the spectra of *p*-ATP on the Ag NP modified glass, which illustrates that Ag NPs can enhance the molecules below it because of the electromagnetic coupling between Au and Ag NPs, and the spectra features of the molecules are not changed greatly. The slight shift of the vibration bands in two sandwich structures may be derived from a slight titled orientation of *p*-ATP with respect to the surface of the Ag NPs such as ν_{CC}(1584–1576 cm^{-1}).[32] Assignments and wave number positions for the Raman spectrum of the solid *p*-ATP and the SERS spectra of *p*-ATP are listed in Table I.

CONCLUSIONS

Sandwich structures of Ag NPs/*p*-ATP SAMs/Ag NPs and Au NPs/*p*-ATP SAMs/Ag NPs are fabricated successfully on glass and investigated by SERS. The EF values at a single Ag-to-Ag NPs sandwich structure are as large as $6.0\pm0.62\times10^4$ and $1.2\pm0.62\times10^7$ for $7a$ and $3b(b_2)$ vibration modes of *p*-ATP, respectively, suggesting the strong electromagnetic coupling effect between the two layers of Ag NPs, most probably due to the interaction of the LSP of the Ag NPs. Large EF values ($1.9\pm0.7\times10^4$ and $9.4\pm0.7\times10^6$ for $7a$ and $3b(b_2)$ vibration modes, respectively) were also obtained for solely one sandwich structure of Au NPs/*p*-ATP SAM/Ag NPs, which clearly indicates that the sandwich structure can provide a hot spot for the induction of SERS via the electromagnetic coupling between two layers of metal NPs.

ACKNOWLEDGMENT

This work was supported by the National Natural Sciences Foundation of China projects (Nos. 20275037 and 20210506)

[1] M. Fleischmann, P. J. Hendra, and A. J. Mcquillan, Chem. Phys. Lett. **26**, 163 (1974).
[2] F. Ni and T. M. Cotton, Anal. Chem. **58**, 3159 (1986).
[3] M. M. Carrabba, R. B. Edmonds, and R. D. Rauh, Anal. Chem. **59**, 2559 (1987).
[4] N. S. Lee, Y. Z. Hsieh, R. F. Paisley, and M. D. Morris, Anal. Chem. **64**, 442 (1988).
[5] R. L. Garrell, Anal. Chem. **61**, 401A (1989).
[6] M. Futamata, Y. Maruyama, and M. Ishikawa, J. Phys. Chem. B **108**, 13119 (2004).
[7] L. Bao, S. M. Mahurin, R. G. Haire, and S. Dai, Anal. Chem. **75**, 6614 (2003).
[8] D. H. Jeong, Y. X. Zhang, and M. Moskovits, J. Phys. Chem. B **108**, 12724 (2004).
[9] P. A. Mosier-Boss and S. H. Lieberman, Anal. Chem. **77**, 1031 (2005).
[10] Y. Sun, B. Wiley, Z.-Y. Li, and Y. Xia, J. Am. Chem. Soc. **126**, 9399 (2004).
[11] R. M. Jarvis and R. Goodacre, Anal. Chem. **76**, 40 (2004).
[12] R. M. Jarvis, A. Brooker, and R. Goodacre, Anal. Chem. **76**, 5198 (2004).
[13] F. Yu, B. Persson, S. Lofas, and W. Knoll, Anal. Chem. **76**, 6765 (2004).
[14] S. M. Barnett, B. Vlckova, I. S. Butler, and T. S. Kanigan, Anal. Chem. **66**, 1762 (1994).
[15] M. Kahl and E. Voges, Phys. Rev. B **61**, 14078 (2000).
[16] V. M. Shalaev and A. K. Sarychev, Phys. Rev. B **57**, 13265 (1998).
[17] M. Moskovits, D. P. Dilella, and K. L. Maynard, Langmuir **4**, 67 (1988).
[18] L. Y. Cao, P. Diao, L. M. Tong, T. Zhu, and Z. F. Liu, ChemPhysChem **6**, 913 (2005).
[19] H. Ueba, Surf. Sci. **131**, 347 (1983).
[20] A. Otto, J. Billmann, J. Eickmans, U. Erturk, and C. Pettenkofer, Surf. Sci. **138**, 319 (1984).
[21] J. F. Arenas, M. S. Woolley, J. C. Otero, and J. I. Marcos, J. Phys. Chem. **100**, 3199 (1996).
[22] K. L. Kelly, E. Coronado, L. L. Zhao, and G. C. Schatz, J. Phys. Chem. B **107**, 668 (2003).
[23] M. A. El-Sayed, Acc. Chem. Res. **34**, 257 (2001).
[24] R. G. Freeman, K. C. Grabar, K. J. Allison *et al.*, Science **267**, 1629 (1995).
[25] S. M. Nie and S. R. Emery, Science **275**, 1102 (1997).
[26] A. M. Michaels, J. Jiang, and L. Brus, J. Phys. Chem. B **104**, 11965 (2000).
[27] M. Kahl and E. Voges, Phys. Rev. B **61**, 14078 (2000).
[28] V. M. Shalaev and A. K. Sarychev, Phys. Rev. B **57**, 13265 (1998).
[29] T. Hayakawa, S. T. Selvan, and M. Nogami, Appl. Phys. Lett. **74**, 1513 (1999).
[30] A. Campion and P. Kambhampati, Chem. Soc. Rev. **27**, 241 (1998).
[31] M. Moskovits, Rev. Mod. Phys. **57**, 783 (1985).
[32] J. W. Zheng, Y. G. Zhou, X. W. Li, Y. Ji, T. H. Lu, and R. A. Gu, Langmuir **19**, 632 (2003).
[33] C. J. Orendorff, A. Gole, T. K. Sau, and C. J. Murphy, Anal. Chem. **77**, 3261 (2005).
[34] K. Kim and J. K. Yoon, J. Phys. Chem. B **109**, 20731 (2005).

[35] K. Kim and H. S. Lee, J. Phys. Chem. B **109**, 18929 (2005).
[36] C. D. Keating, K. K. Kovaleski, and M. J. Natan, J. Phys. Chem. B **102**, 9414 (1998).
[37] C. E. Taylor, J. E. Pemberton, G. G. Goodman, and M. H. Schoenfisch, Appl. Spectrosc. **53**, 1212 (1999).
[38] R. G. Freeman, M. B. Hommer, K. C. Grabar, M. A. Jackson, and M. J. Natan, J. Phys. Chem. **100**, 718 (1996).
[39] L. Rivas, S. Sanchez-Cortes, J. V. Garcia-Ramos, and G. Morcillo, Langmuir **16**, 9722 (2000).
[40] P. C. Lee and D. Meisel, J. Phys. Chem. **86**, 3391 (1982).
[41] M. Moskovits and J. S. Suh, J. Phys. Chem. **88**, 5526 (1984).
[42] M. Osawa, N. Matsuda, K. Yoshii, and I. Uchida, J. Phys. Chem. **98**, 12702 (1994).
[43] J. W. Zheng, X. W. Li, Y. Ji, R. A. Gu, and T. H. Lu, J. Phys. Chem. B **106**, 1019 (2002).
[44] A. Vivoni, S. P. Chen, D. Ejeh, and C. M. Hosten, Langmuir **16**, 3310 (2000).
[45] K. Carron and L. G. Hurley, J. Phys. Chem. **95**, 9979 (1991).
[46] H. J. Chen, Y. L. Wang, S. J. Dong, and E. K. Wang, Spectrochim. Acta, Part A **64**, 343 (2005).
[47] K. V. G. K. Murty, M. Venkataramanan, and T. Pradeep, Langmuir **14**, 5446 (1998).
[48] J. Wang, T. Zhu, and Z. F. Liu, Acta Phys.-Chim.Sin. **14**, 485 (1998).
[49] Q. J. Huang, B. W. Mao, R. A. Gu, and Z. Q. Tian, Chem. Phys. Lett. **271**, 101 (1997).
[50] Q. J. Huang, X. Q. Li, J. L. Yao, B. Ren, W. B. Cai, J. S. Gao, B. W. Mao, and Z. Q. Tian, Surf. Sci. **427/428**, 162 (1999).
[51] J. F. Arenas, I. Lopez-Tocon, J. L. Castro, S. P. Centeno, M. R. Lopez-Ramirez, and J. C. Otero, J. Raman Spectrosc. **36**, 515 (2005).
[52] L. Gunnarsson, E. J. Bjerneld, H. Xu, S. Petronis, B. Kasemo, and M. Kall, Appl. Phys. Lett. **78**, 802 (2001).
[53] B. Ren, X. F. Lin, Z. L. Yang, G. K. Liu, R. F. Aroca, B. W. Mao, and Z. Q. Tian, J. Am. Chem. Soc. **125**, 9598 (2003).
[54] W. B. Cai, B. Ren, X. Q. Li, C. X. She, F. M. Liu, X. W. Cai, and Z. Q. Tian, Surf. Sci. **406**, 9 (1998).
[55] A. Otto, I. Mrozek, and C. Pettenkofer, Surf. Sci. **238**, 192 (1990).
[56] P. He, H. Liu, Z. Li, Y. Liu, X. Xu, and J. Li, Langmuir **20**, 10260 (2004).
[57] http://www.chemicaland21.com/life science/phar/4-aminothiophenol.htm